TAGA Proceedings, 1995 - Volume 1

Application of Turbid Medium Theory to Paper Spread Function Measurements

Peter G. Engeldrum and Brian Pridham*

KEYWORDS: Optics, Paper, Image Quality, Microdensitometry,

ABSTRACT

It is becoming increasingly important in printing systems to expand the accuracy of imaging models; e.g., Neugebauer and structured dot. More complex models must ultimately include the spread of light within the paper structure (paper optical spread function). Paper makers have successfully used Kubelka-Munk (K-M) turbid medium theory for defining the tradeoffs of paper properties such as opacity and reflectivity. A theoretical analysis and a series of measurements are described that relates the scattering and absorbing coefficients, K and S, from the K-M theory to paper spread functions and their Fourier Transforms, the paper "MTF." The results show that the paper MTFs of coated papers, not conforming to the assumptions of K-M theory, are poorly described by the theoretical MTF. So called "plain papers," such as newsprint, copying and typewriter bond, are well described by the K-M MTF at low spatial frequencies.

INTRODUCTION

For decades it has been known that when the same halftone printing plate is printed on different papers, the resulting average print reflectances, or tone reproduction curves, are different[(1)]. The main reason for this phenomenon

* Peter Engeldrum is president of Imcotek, POB 17 Winchester, MA 01890, E-mail: Imcotek@aol.com. Brian Pridham is currently with the Eastman Kodak Co., Rochester, NY. Some of this work was performed while the authors were associated with the Center for Imaging Science at the Rochester Institute of Technology, Rochester, NY.

is the scattering of light within the paper substrate, the so-called Yule-Neilsen effect[2].

The paper scatters light largely because of the refractive index mismatch between the air or binder, and the fibers or other paper constituents. A consequence of scattering is the variety of path lengths that the light takes before it emerges from the paper. Some light emerges a very short distance from where it entered and some emerges at some greater distance. Light that enters a space in the halftone pattern exits through a dot, and is absorbed. An increase in absorption results in a measured decreased of reflectance, or an apparent dot area increase from what would be expected based solely on fractional dot area considerations. Recent measurements on halftone patches from a color wax thermal transfer printer show that both dot and paper reflectance factors depend on fractional area covered[3]. This phenomenon is not limited to printing, it occurs with many other imaging systems that use halftones to produce images[4], and is a factor in optical radiation measurements[5] and reflection microdensitometry[6].

The spatial scattering properties can be summarized as the paper reflectance line or point spread function, analogous to the more familiar spread function of lenses and photographic materials. Several mathematical models have been suggested to describe the spread functions of paper. Yule et. al.[7] measured reflectance edge gradients of a series of unprinted paper samples. Their conclusion was that the line spread functions, the derivatives of the measured edge gradients, were Gaussian shaped. Measurements by Wakeshima, et. al.[8] suggest that the point spread function is radially exponential. It can be shown, but we will not do so here, that the exponential *point* spread function of Wakeshima et. al. and the Gaussian *line* spread function of Yule et. al. are difficult to distinguish when determined from edge gradient measurements. The difference between the two functional forms can be easily obscured by the noise of such measurements.

A theoretical framework for paper spread functions would be very useful for both the paper designer-manufacturer and the imaging systems engineer. Such a framework would allow the *a priori* design of the paper spread function such that the optimum image quality would result for any given imaging technology. Paper designers have found the Kubelka-Munk turbid scattering theory[9] useful in selecting paper constituents to achieve certain reflectivity and opacity properties. The K-M theory is attractive on two counts. The first is its two parameter formalism, the absorbing coefficient, K, and the scattering coefficient, S. Secondly, the two parameters, K and S, can be determined from two reflectance measurements, one over a black backing of zero reflectance and one over a white backing of known reflectance. The

simple K-M theory assumes a homogenous absorber-scatterer that is not, in principle, obeyed by coated papers.

Kubelka-Munk theory has been tied to halftone imaging for at least 35 years. In 1960, Jorgensen[10] used the K-M scattering parameter, S, to describe the contrast of a bar pattern printed on various papers. For a fixed spatial frequency, cy/mm, he found that the density difference between the bars and the paper between the bars was related to the square root of S. Jorgensen's work[10] has established a relationship between the K-M scattering coefficient and some measure of the effect of paper spread function, the printed image contrast or density difference. More recently, Oittinen[11] has suggested that the derivative of the basic K-M reflectance equation can be used as a point spread function for paper. Both the work by Jorgensen and Oittinen, and the established practical application of K-M in the paper industry, suggests that we might be successful in determining the paper reflectance spread function, or its equivalent Fourier Transform ("MTF"), using simple methods for determining K and S.

Our specific objective was to measure the paper reflectance line spread function, compute its Fourier transform, FT, and relate the measured FT to the theoretical FT whose parameters were determined from simple large area reflectance measurements.

THEORY

In this section we derive the complete point spread function, PSF, the Fourier transform or the so-called paper MTF, and the line spread function, LSF, all from the K-M theory.

K-M Point Spread Function

The basic equation relating the reflectance of a homogenous absorbing-scattering medium as a function of the backing reflectance, R_g, and the Reflectivity, R_∞, scattering coefficient, S, and distance, r, is as follows[9]: Although the absorption coefficient, K, is not explicit in equation (1), it is implicitly in R_∞ according to the relationship, $K/S = (1-R_\infty)^2/2R_\infty$.

If we set $R_g = 0$ and differentiate equation (1) with respect to the distance, r, we have after some manipulation the point spread function given by equation (2)[11];

$$s(r) = \frac{S\left(1 - R_\infty^2\right)^2 e^{-2bSr}}{\left(1 - R_\infty^2 e^{-2bSr}\right)^2} \qquad (2)$$

where 2b = ($1/R_\infty$ - R_∞). [Using the definition of K-M transmittance, the spread function given by equation (2) can be shown to be proportional to the square of the transmittance. This suggests an alternative, and perhaps simpler, method for determining the reflectance spread function.] By expanding the denominator of equation (2) in a power series, and taking only the first term, we have the *approximate* point spread function, s*(r), given by equation (3).

$$s*(r) = S\left(1 - R_\infty^2\right)^2 e^{-2bSr} \qquad (3)$$

Note that the PSF described by equation (3) is exponential in form and is in accord with the observations of Wakeshima, et. al.[8]. Figure 1 illustrates the PSF given by equation (2) for bounding values of K and S that were found in our paper samples. The PSF's are all normalized to unity at the origin. Many shapes are illustrated in figure 1. Under one condition, K=3, S=10 and R_∞=0.469, the PSF is almost exponential, but would have a gray appearance. Other combinations of K and S produce shapes that are similar to those reported by Lehmbeck et. al.[6]

Figure 1. K-M Point Spread Functions

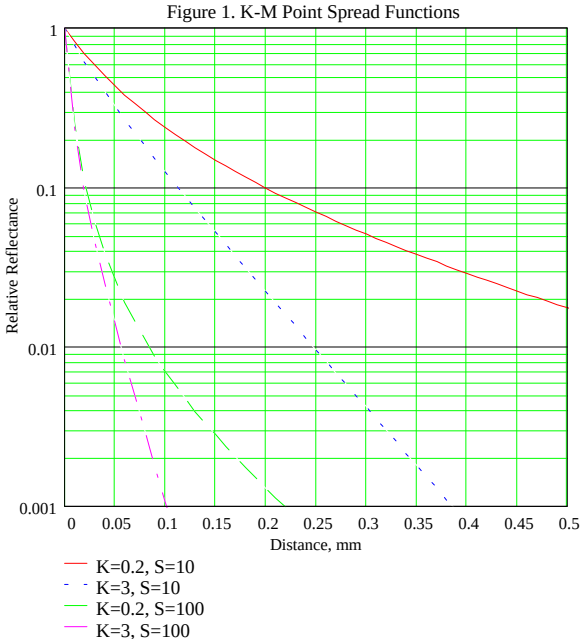

Fourier Transform - MTF

Two other forms of the paper point spread function are of interest. The first is the Fourier transform of equation (2), and the second is the line spread function, LSF, or the one dimensional version of equation (2).

We see from equation (2) that the PSF depends on the radius, r, only; i.e., rotationally symmetric. In this circumstance we can take the Hankel transform of (3) to get the MTF instead of the two dimensional Fourier transform. The Hankel transform[13] is given by equation (4);

$$T(\omega) = \int_0^{\infty} s(r)\, J_0(2\pi\omega r) r dr \qquad (4)$$

where ω = spatial frequency, cy/mm. Combining equations (2) and (4), and some tedious algebra, we have equation (5), the paper "MTF."

$$T(\omega) = \frac{1}{\ln\left(\frac{1}{1-R_\infty^2}\right)} \sum_{k=1}^{\infty} \frac{R_\infty^{2k}}{k} \left[1 + \left(2\pi \frac{\omega}{2bSk}\right)^2\right]^{-\frac{3}{2}} \qquad (5)$$

Figure 2 shows equation (5) for our select values of K and S. Note that as S increases, the MTF increases; i.e., becomes flatter. Thus increasing S is a route to narrower spread functions and high reflectance factor, for constant K.

Figure 2. Paper "MTFs"

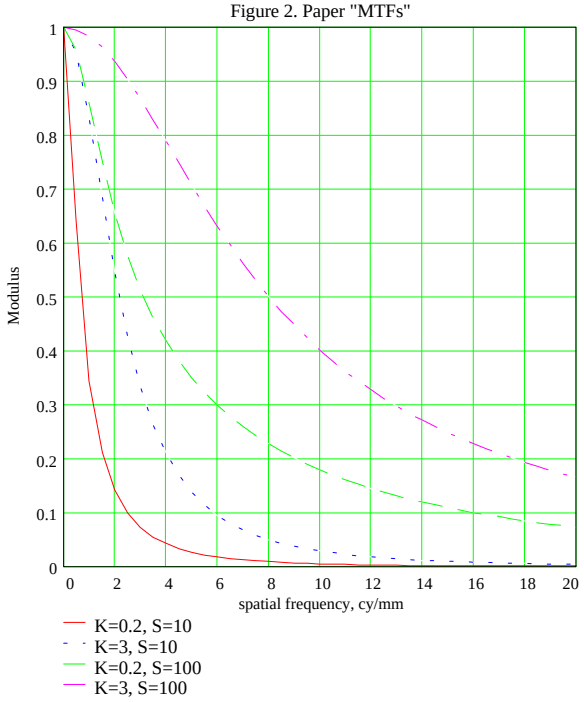

Line Spread Function

Experimentally, the line spread function, LSF, is the simplest to measure and there are two approaches to defining it theoretically; equations (6a, 6b).

$$l(x) = \int_{-\infty}^{+\infty} s(x,y)dy \qquad (6a)$$

$$l(x) = \int_{-\infty}^{+\infty} T(\omega)\cos(2\pi\omega x)d\omega \qquad (6b)$$

Equation (6b) is just the Fourier Transform of the MTF, equation (5), and we choose this route to the line spread function. By substituting equation(5) into equation (6b) and doing the integration, the K-M LSF is given by equation(7);

$$l(x) = \frac{2bS}{\pi \ln\left[\frac{1}{1 - R_\infty^2}\right]} \sum_{j=1}^{\infty} R_\infty^{2j} \left(j2bS|x|\right) K_1(j2bS|x|) \qquad (7)$$

where $K_1()$ is a modified Bessel function of the first kind and order one. Figure 3 is a plot of equation (7) for the same values of K and S used the PSF and the MTF. Note that the LSFs are wider than their corresponding point spread functions shown in Figure 1.

Figure 3. K-M Line Spread Functions

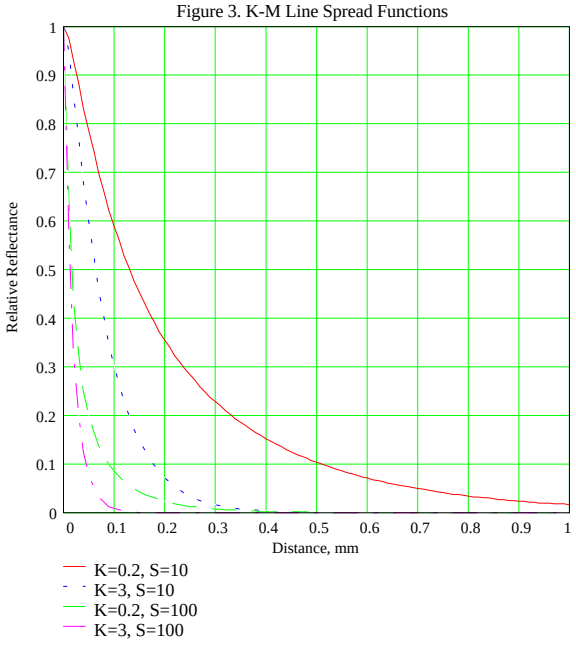

EXPERIMENTAL

Paper Samples

The selection of ten papers for this investigation was largely arbitrary. However, the emphasis was on "imaging" papers that included coated ink jet, cast coated printing papers, newsprint, copy and typewriter papers. Our goal was to include a sufficient variety of papers so we could determine the robustness of the K-M formalism as a spread function model. Table I summarizes the paper samples along with their measured characteristics; basis weight, thickness, and Kubelka-Munk K and S values.

Table I Paper Sample Summary

Sample ID	Paper Type	Basis Wt, gr/m^2	Thickness, mm	K, mm^{-1}	S, mm^{-1}
1	Ink jet - MIJD	48	0.0889	0.226	42.7
2	Ink jet - ACT	67	0.112	0.315	28.2
3	Vintage Gloss	104	0.0914	0.811	92.9
4	Lustercoat	203	0.269	0.467	41.5
5	Javelin	95	0.0864	0.820	63.9
6	Vintage Gloss	270	0.269	0.365	52.5
7	Javelin	115	0.119	0.604	48.0
8	Newsprint	38	0.104	2.65	22.1
9	Copy Paper	65	0.114	0.535	29.8
10	Typewriter Bond	62	0.125	0.413	29.4

In calculating the K-M absorbing, K, and scattering, S, parameters we followed the method outlined in reference (9). The reflectance of each sample was measured with a microdensitometer, through a green filter (Wratten #58). The first measurement was made over a white background of 0.863 visual reflectance factor, and the second over a black background of <0.001 reflectance factor. The optical geometry was annular illumination, at 45^o from the normal, and normal collection of the reflected flux. This differs from the

K-M model of totally diffuse illumination and collection. However, Kubelka[14] suggests that these geometry differences cause the K and S values to scale by a factor under certain conditions.

Sample thickness was determined with a micrometer using ten sheets to average out any individual sheet differences. K and S coefficients were calculated for each sample using the following set of equations[9].

$$a = \frac{1}{2}\left[R + \frac{\left(R_0 - R + R_g\right)}{R_0 R_g}\right] \qquad (8a)$$

$$b = \sqrt{a^2 - 1} \qquad (8b)$$

$$SX = \frac{1}{b}\ln\left[\coth^{-1}\left(\frac{a - R}{b}\right) - \coth^{-1}\left(\frac{a - R_g}{b}\right)\right] \qquad (8c)$$

$$K = S(a - 1) \qquad (8d)$$

Where R = reflectance factor of the paper over a white backing, R_0 = the reflectance factor of the paper over a black (zero reflectance factor) backing, R_g = reflectance of the white backing, X = paper thickness, mm, and $\coth^{-1}()$ = inverse hyperbolic cotangent.

Edge Projector

Edge gradient measurements were made using the same technique described by Yule, et. al.[7] using a photographic knife edge projector (see figure 4). Briefly, a 10:1 contrast knife edge, printed on a very high resolution photographic film, was projected by an inverted microscope system. In this system the edge is placed where the eye piece is

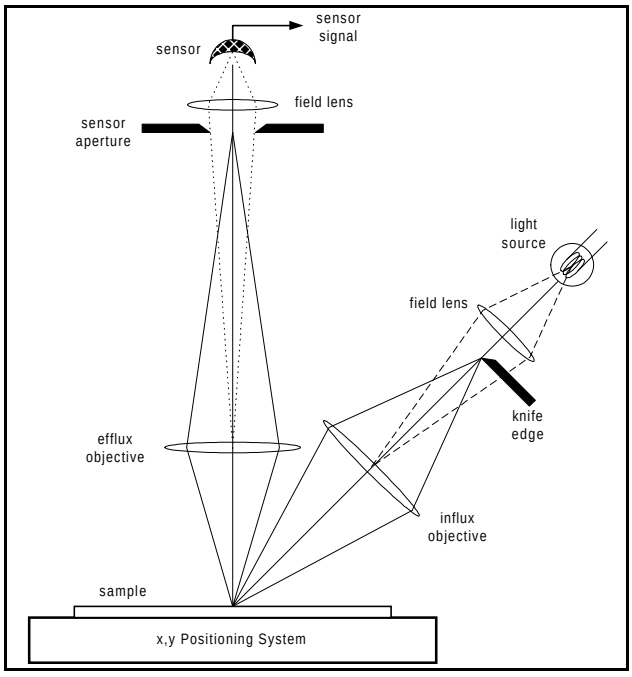

Figure 4 - Edge Projector Schematic

normally positioned. The projected image is a reduced version of the physical edge that depends on the magnification of the objective lens. This technique projects a high quality edge limited by the optics of the microscope, a 0.08 numerical aperture, NA, objective in our case. Any residual chromatic aberration in the microscope objective was reduced by filtering the projected light by a green (Wratten #58) filter. Filtering the tungsten filament light source in this way also removed any UV radiation that could excite brighteners in the papers. The edge projector was at a 45-degree angle to the paper surface. Focusing of the projected edge was achieved by moving the complete microscope assembly along this 45-degree line.

A computer controlled reflection microdensitometer was used to measure the reflectance edge gradients by moving the edge, projected on the paper sample, past the measuring slit. Motion of the edge was accomplished by fastening the edge projector to the computer controlled x-y positioning system of the microdensitometer. The microdensitometer had an effective scanning slit aperture of 25.4µm x 1000µm, with a lens NA of 0.10. Under these conditions the optical performance of the microdensitometer was effectively diffraction limited. All papers were backed up with a 0.827 visual reflectance factor white metal platen.

Data Collection and Reduction

Reflectance factor readings of the edge projected onto a single sheet of paper were taken at 12.7µm intervals. This was the smallest interval possible with the microdensitometer x-y positioning system. At every position, ten readings were time-averaged to reduce the electrical noise of the instrument. This strategy left only the image noise associated with the paper surface reflectance. The sequence of edge reflectance factor measurement comprised the edge data. Typically an edge trace length was about 70 points, or 0.9mm. Determining the trace length was done visually from a plot of reflectance factor versus distance. Data trace ends were identified when the reflectance factors became constant, or approximately so, at either side of the edge. The slopes at the ends of the edge data were very low so considerable judgement was called for in determining where the data ended.

Line spread functions were computed by numerically differentiating the edge traces by taking the difference between adjacent data points. The resultant data set was padded with zeros out to 84 points, the maximum trace length. This was done to keep the spatial frequency interval in the MTF calculation a constant. Discrete Fourier transformation of the line spread function data, followed by the calculation of the modulus made up the measured paper "MTF." All calculations were performed using the Windows version of MathCad 5.0+ mathematical software package[12].

RESULTS AND DISCUSSION

Edge Gradients

The measured edge gradients are shown in figures 5.1 and 5.2. On this scale they all appear similar in their rate of change from a reflectance factor of about 0.10 to the bulk paper reflectance. Close inspection of the figure reveals that the noise, or lack of trace uniformity, is greater on the high reflectance side than the low reflectance side. This suggests that the fluctuations are due to the microscopic reflection factor variation. Lack of fluctuations in the edge gradient itself points to spatially band limited noise, roughly the edge gradient extent.

Figure 5.1 Measured Paper Edge Gradient

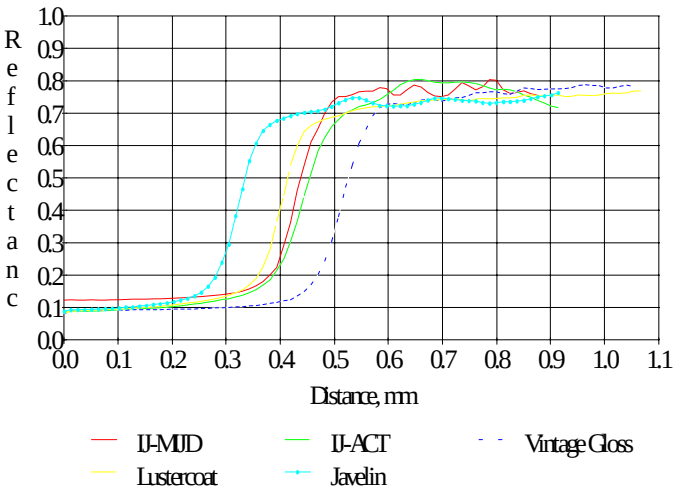

Image noise can be reduced by incorporating a larger area for the spread function measurements. Our hardware did not permit us to do this, and we were limited to measuring an area of 1mm^2. This is too small an area for reliable measurements. Microscopic variations in paper formation would suggest even larger areas, or greater sample numbers, to characterize a specific paper. We think that at least a 30 fold increase in area should be used for these measurements, from both the surface structure and bulk paper properties points of view.

Figure 5.2 Measured Paper Edge Gradient

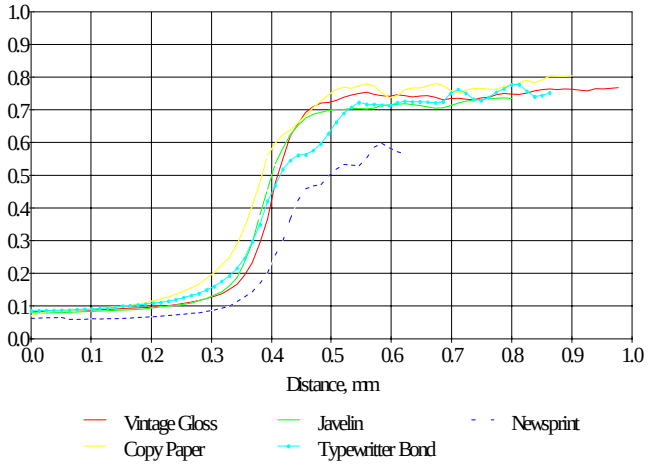

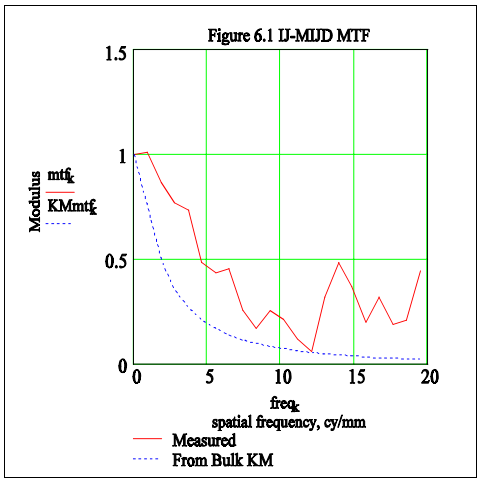

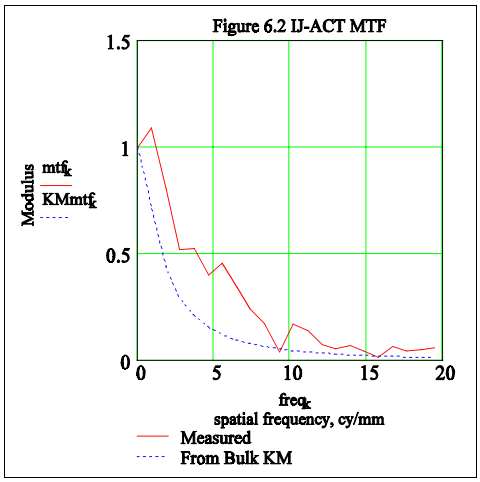

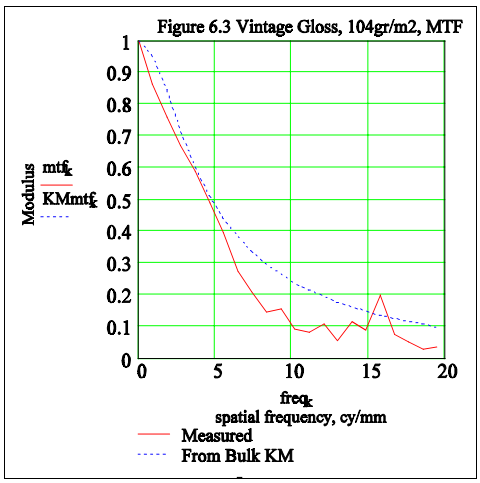

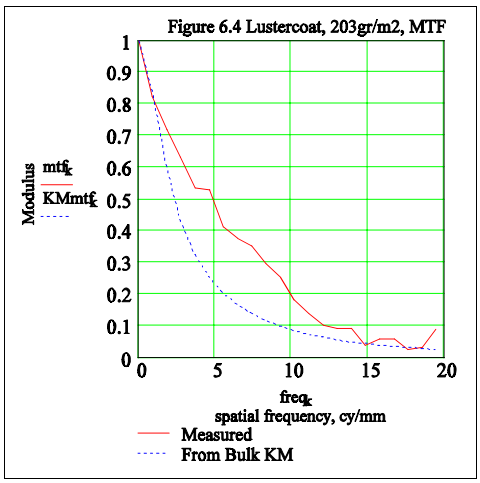

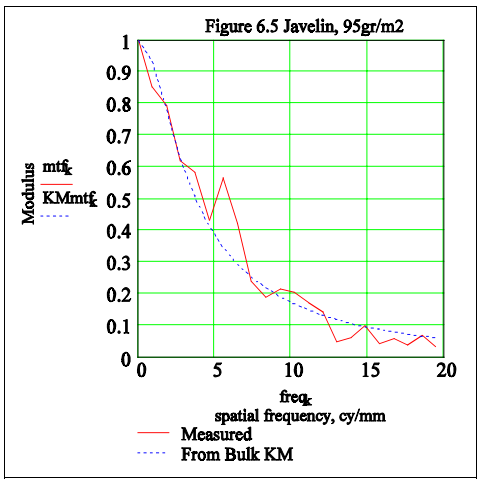

Paper MTF's

Figures 6.1 - 6.10 show the comparisons between the measured MTF and the theoretical MTF. The theoretical MTF was calculated from equation (5) using the data for all of the papers listed in table 1.

An obvious goodness-of-fit metric between measurement and theory is the root-mean-square, RMS, deviation. Due to the high image noise an RMS summary measure does not

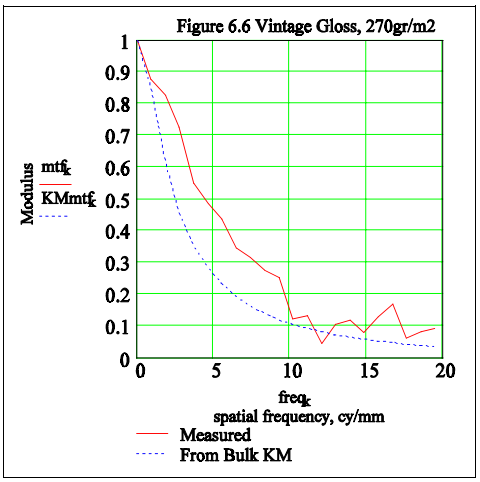

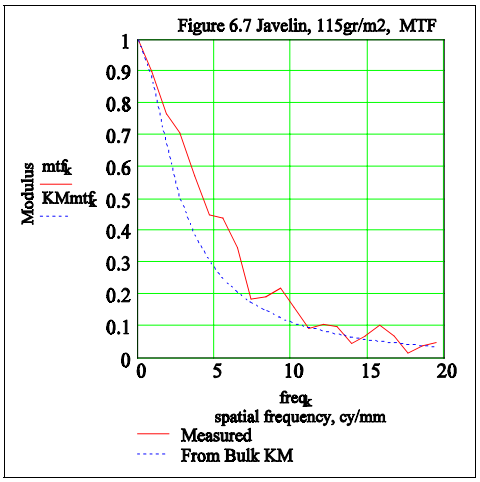

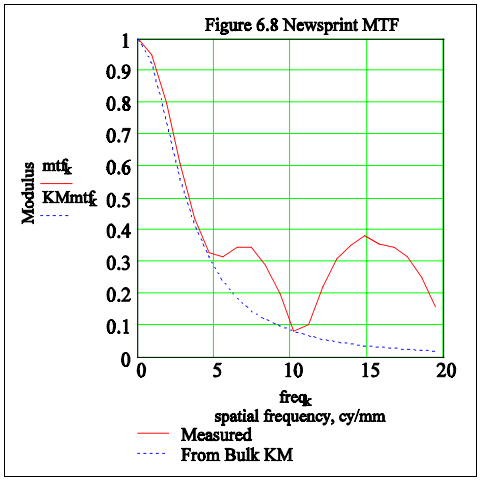

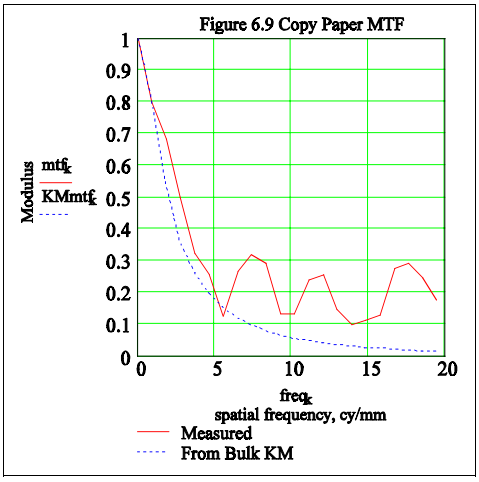

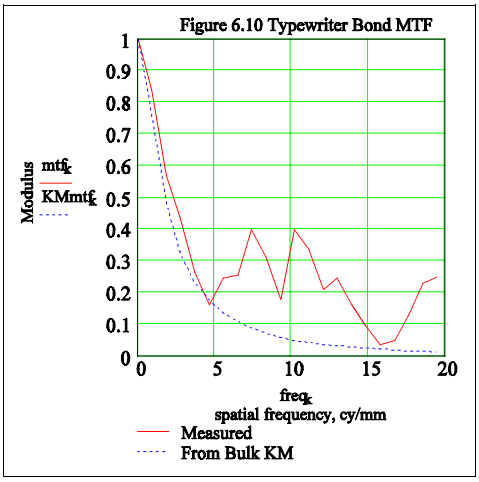

adequately capture the goodness-of-fit of the data to the K-M model.

Two papers, Javelin and Vintage Gloss are represented at two basis weights. The measured MTFs for the Vintage gloss, Figures 6.3 and 6.6, and Javelin, Figures 6.5 and 6.7, show small differences, but the differences in the theoretical MTFs are substantial. Lower basis weight coated papers seem to follow the K-M model better than higher basis weight coated papers. An exception

to this is the ink jet papers, Figures 6.1 and 6.2. The theory did a poor job of predicting the measurements for these coated papers, particularly the rise in MTF at 0.5cy/mm.

For so-called "plain papers" the agreement between theory and measurements at low spatial frequencies was very good. (See figures 6.8 - 6.10.) This might be expected since these papers are closer to the assumptions of the K-M model. At the higher spatial frequencies the noise in the measured MTF makes comparison almost impossible. However, at higher spatial frequencies the predicted MTF usually is less than the measured value. This result would be anticipated if random noise were added to the edge gradient, because the modulus is positively biased by an amount that depends on the noise Wiener spectrum.

The general rule, from these results, may be that the papers with simple structure, the uncoated papers, obey the model quite well. Coated papers, although not expected to follow the K-M model because of the layered construction, are only sometimes accurately represented by the K-M theory.

Recall that the MTF described by equation (5) is for $R_g = 0$. Our measurements did not conform to that assumption. We used a white backing instead of a zero reflectance backing. However, for most of the samples we are not far from the optical configuration where the paper is at R_∞. Thickness ranges required to achieve the opaque case varies from approximately 0.24mm to 0.67mm for our samples. We would expect the paper spread function to be wider since the transmitted light has an opportunity to reflect off the white platen backing and back into the paper. The paper MTF would correspondingly decrease with frequency, so the K-M model may overestimate the paper MTF for the single sheet case.

A useful comparison of theory to measurements hinges on the knowledge of the measured values of K and S for the paper. In our case we used the approximately equivalent optical illumination geometry (influx geometry) for both the K and S measurements and the edge gradients so the parameters for the MTF calculations are comparable. Microscopic variations in paper formation leads to spatial variations in K and S. The variance in these quantities and how they influence the paper MTF awaits further study.

CONCLUSIONS

For simple, uncoated, paper the MTF from the infinite thickness K-M model is an excellent first order estimate of the paper MTF when using K and S determined from large area (bulk properties) reflectance factor measurements. The MTF's of coated papers are generally not well fit by K-M theory, probably due to lack of conformance to model assumptions. The noise in the

edge gradient method using a measurement slit length of 1.0mm is not low enough for accurate (noise free) determination of the paper MTFs. The edge gradient method needs to include at least 30 times larger area in the measurement for satisfactory data.

REFERENCES

1) Yule, J.A.C., *Principles of Color Reproduction*, Chapter 7, J. Wiley & Sons, New York 1967
2) Yule, J.A.C. & J. W. Nielsen, TAGA Proceedings, 1951, pp65-76.
3) Engeldrum P., Jour. Imag. Sci. & Tech., 23:545(1994)
4) Zeng, H., J. Arney & P. Engeldrum, TAGA Proceedings, 1995
5) Hsia, J., NBS Technical Note 594-12, 1976. (NBS is now known as NIST)
6) Lehmbeck, D., J. J. Jakubowski, Jour. Appl. Photo. Eng. 5:63(1979)
7) Yule, J. A. C., D. Howe, & J. Altman, TAPPI, 50:337(1967)
8) Wakeshima, H., T. Kunishi & S. Kaneko, Jour. Opt. Soc. Amer., 58:272(1968)
9) Judd, D. B. & G. Wyszecki, *Color in Business, Science and Industry*, J. Wiley & Sons, NY, 1975, pp 420-438.
10) Jorgensen, G. *Research Progress*, 47:1(1960), Graphic Arts Technical Foundation, Pittsburgh, PA.
11) Oittinen, P., in *Advances in Printing Science and Technology*, W. H. Banks Ed., Pentech Press, London, UK, 1982, Vol 16 pp121-128
12) Available from MathSoft Inc., 101 Main Street, Cambridge, MA 02142
13) Dainty, C. & R. Shaw, *Image Science*, Chapter 6, Academic Press, New York, 1974
14) Kubelka, P., Jour. Opt. Soc. Amer. 448:38(1948)